

METHANE INDEX: A TETRAETHER ARCHAEAL LIPID BIOMARKER PROXY FOR
DETECTING THE INSTABILITY OF MARINE GAS HYDRATES

by

YIGE ZHANG

(Under the Direction of Chuanlun L. Zhang)

ABSTRACT

Gas hydrates are one of the largest pools of readily exchangeable carbon on Earth surface. Releases of the greenhouse gas methane from hydrates are responsible for a number of important climate changes in geological history. Many of the inferred events were based on the $\delta^{13}\text{C}$ values of carbonates, which have been challenged lately. Here we propose a molecular fossil proxy “Methane Index (MI)” to better document the destabilization of marine gas hydrates. MI is constructed by the relative distribution of glycerol dialkyl glycerol tetraethers (GDGTs), the core membrane lipids of *Archaea*. Our study in the Gulf of Mexico sediments clearly shows the correlation between gas venting, microbial community and lipid profile shifts and the MI, corroborating the idea that MI might be a robust indicator for hydrate dissociation. MI provides us a more precise and effective proxy for evaluating the gas hydrate instability in Earth’s geological history.

INDEX WORDS: Methane Index; Gas Hydrate; Gulf of Mexico, *Archaea*, GDGTs

METHANE INDEX: A TETRAETHER ARCHAEAL LIPID BIOMARKER PROXY FOR
DETECTING THE INSTABILITY OF MARINE GAS HYDRATES

by

YIGE ZHANG

BS, Nanjing University, China, 2007

A Thesis Submitted to the Graduate Faculty of The University of Georgia in Partial Fulfillment
of the Requirements for the Degree

MASTER OF SCIENCE

ATHENS, GEORGIA

2009

© 2009

YIGE ZHANG

All Rights Reserved

METHANE INDEX: A TETRAETHER ARCHAEAL LIPID BIOMARKER PROXY FOR
DETECTING THE INSTABILITY OF MARINE GAS HYDRATES

by

YIGE ZHANG

Major Professor: CHUANLUN L. ZHANG

Committee: JOHN E. NOAKES
MING-YI SUN

Electronic Version Approved:

Maureen Grasso
Dean of the Graduate School
The University of Georgia
August 2009

DEDICATION

This thesis is dedicated to my parents, Jianxing Zhang and Ling Liu, my grandmother, Yushan Chen, and my fiancée, Ping Hu, for their support and love for all those years.

ACKNOWLEDGEMENTS

First I would like to thank my advisor, Dr. Chuanlun Zhang, for the tremendous advice, support, and guidance he has offered throughout my thesis studies. He is so nice as a person, his care, understanding and help in various ways made me able to go through obstacles and making progress all along the way.

I also appreciate the assistance and support I received from my thesis committee, Dr. John Noakes and Dr. Ming-Yi Sun. Dr. Wei-Jun Cai and Dr. Chris Romanek also helped me both inside and outside the classrooms.

Marshall Bowles helped with sample collection. Hai Pan, Kathy Bowles and Wei-Jen Huang offered technical support. Dr. Li Li at Tongji University helped with stable isotope analysis. Xiaolei Liu and Dr. Kai-Uwe Hinrichs at the University of Bremen helped with HPCL-MS and GC-IRMS analysis. I thank Xinping Hu for stimulating discussion.

Finally, I acknowledge financial support by the University of Mississippi Gulf of Mexico Hydrates Research Consortium with funding from the Minerals Management Service of the Department of the Interior, the National Energy Technology Laboratory of the Department of Energy and the National Institute for Undersea Science and Technology of the National Oceanographic and Atmospheric Administration of the Department of Commerce, and by a Geological Society of America student research grant.

TABLE OF CONTENTS

	Page
ACKNOWLEDGEMENTS	v
LIST OF TABLES	viii
LIST OF FIGURES	ix
CHAPTER	
1 Introduction.....	1
Gas hydrates and Methane Triggered Climate Changes	1
Archaea, Methanotrophic Archaea and Their Lipids	4
2 Literature Review.....	7
GDGT Distribution in Normal Marine Environments	7
GDGT Distribution in Gas Hydrate Impacted Environments	15
3 Gas Hydrate Impacted Environments in the Gulf of Mexico: A Natural Laboratory for Methane Index Studies	19
Materials.....	19
Pore Water Chemistry	25
Stable Isotope for Carbonates.....	25
Lipid Analysis	25
GDGT Cleavage and Compound Specific Isotope Analysis.....	27
4 Results and Discussion	29
Pore Water Chemistry and Carbonate Isotope	29

Archaeal Lipids	36
Methane Index: Definition and Verification	42
Methane Index vs. Compound-specific carbon isotopes.....	44
Using Methane Index to Identify Hydrate Impacted Environments	49
Application of Methane Index in Environmental Samples	51
5 Concluding Remarks.....	55
REFERENCES	56

LIST OF TABLES

	Page
Table 3.1: Sampling information for Core 08 and Core 10 in MC 118 during the 2008 R/V Pelican cruise.	24
Table 4.1: Pore water chemistry and stable carbon and oxygen isotope data for Core 08 and Core 10.....	31
Table 4.2: Relative abundance of the GDGTs (%) in Core 08 and Core 10, MC 118, Gulf of Mexico.	37
Table 4.3: Methane index, ether cleavage of GDGTs from selected samples and compound-specific $\delta^{13}\text{C}$ of the released phytane and biphytanes.....	46

LIST OF FIGURES

	Page
Figure 1.1 : Composite marine oxygen and carbon isotopes reveal the Paleocene – Eocene Thermal Maximum (PETM) event occurred around ~ 55 Ma	3
Figure 1.2: Basic structures of five common GDGTs: GDGT-0, GDGT-1, GDGT-2, GDGT-3 and crenarchaeol.....	5
Figure 2.1: HPLC/MS base peak chromatograms of surface sediment from the Arabian Sea and North Sea.....	8
Figure 2.2: Relationship between the TEX ₈₆ index and annual mean SST from 40 surface sediments collected from 15 different worldwide locations	10
Figure 2.3: Partial HPLC-APCI/MS base peak chromatograms of particulate organic matter derived from the mesocosm tank experiments after incubation at 27°C and 13°C, respectively, for three months.	12
Figure 2.4: Correlation of the incubation series. Black dots represent TEX ₈₆ values from incubation at 27‰ salinity, and gray dots represent TEX ₈₆ values from incubation at 35‰ salinity	13
Figure 2.5: HPLC-APCI/MS peak chromatogram shows the GDGT distribution in different environments	16
Figure 3.1: Map shows the location of Mississippi Canyon Block 118 (MC 118) in the north Gulf of Mexico and northeast of the Mississippi Canyon	21

Figure 3.2: Seafloor imagery of MC 118 shows the sampling site during the April 2008 R/V Pelican cruise.....	23
Figure 4.1: Vertical profile of sulfate, sulfide, and stable carbon isotope for Core 08 (A) and Core 10 (B) in MC 118, Gulf of Mexico.....	33
Figure 4.2: Correlation between carbonate $\delta^{18}\text{O}$ and $\delta^{13}\text{C}$ for Core 08 and Core 10	35
Figure 4.3: HPLC/APCI-MS peak chromatogram of two typical samples: Left panel, Core 08, 61 cm; Right panel, Core 10, 121 cm.....	39
Figure 4.4: Vertical distribution of GDGTs in Core 08 and Core 10, MC 118, Gulf of Mexico ..	41
Figure 4.5: Depth dependent MI for Core 08 and Core 10, MC 118, Gulf of Mexico.....	43
Figure 4.6: Structure shows the biphytane released from ether cleavage of GDGTs: biphytane a (acyclic), b (monocyclic), c (bicyclic) and d (tricyclic)	45
Figure 4.7: Methane index vs. compound-specific ^{13}C from biphytane b, released from the GDGTs collected from Core 08 and Core 10, MC 118, Gulf of Mexico.....	48
Figure 4.8: Methane index vs. $\delta^{13}\text{C}$ plot from a variety of marine environment.....	50
Figure 4.9 Histogram shows the methane index calculated from a number of different marine environments	53

Chapter 1

Introduction

Gas hydrates and methane-Triggered Climate Changes

In marine sediments under a delicate balance of temperature and hydrostatic pressure, methane and water can form crystalline solids, which are called gas hydrates (Jiang et al., 2006). Gas Hydrates occur widely along continental margins in the world's oceans. It is estimated that about 10000 Gt methane carbon is stored in marine gas hydrate reservoirs (Kvenvolden, 1999). Thus, the instability of marine gas hydrates as a source of greenhouse gas is paramount to changes in the Earth's climate. Based on mass balance calculations, Dickens et al. (1995) explained the enigmatic Paleocene - Eocene thermal maximum event (PETM) to be a consequence of 1120 Gt methane released from gas hydrate reservoirs (Fig. 1.1) (Dickens et al., 1995). After this pioneering work, the importance of gas hydrates has been increasingly recognized. For example, gas hydrate dissociation and CH₄ release may have triggered the Cretaceous ocean anoxic events (Wagner et al., 2007), late Jurassic global warming (Padden et al., 2001), and even the Neoproterozoic deglaciation (Jiang et al., 2003).

For the more recent Quaternary Period, A "Clathrate Gun Hypothesis" was proposed which stated that the massive release of CH₄ from marine gas hydrate dissociation led to global, abrupt warming (Kennett et al., 2000; Kennett et al., 2002). However, direct evidence of gas hydrate dissociation and methane release is scarce. For example, most of

the inferred Quaternary methane release events are primarily based on the carbon isotope studies of foraminiferal shells (e.g., de Garidel-Thoron et al., 2004; Kennett et al., 2000; Wang et al., 2008) and methane-release induced carbon isotope negative excursions have been challenged by subsequent studies (Cannariato and Stott, 2004; Stott et al., 2002). Stott and colleagues argued that the vital effect and/or variations of isotopic gradients of dissolved inorganic carbon in pore water in response to varying intensities of microbial remineralization of organic carbon may be responsible for the observed carbonate $\delta^{13}\text{C}$ variations. Thus, a new proxy is needed to unambiguously evaluate the instability of gas hydrates reservoirs in the geological past. Hinrichs et al. (2003) showed that a better evidence may come from the molecular fossils that have been produced by the anaerobic methanotrophic archaea that were directly associated with the cycling of methane in the deep sea.

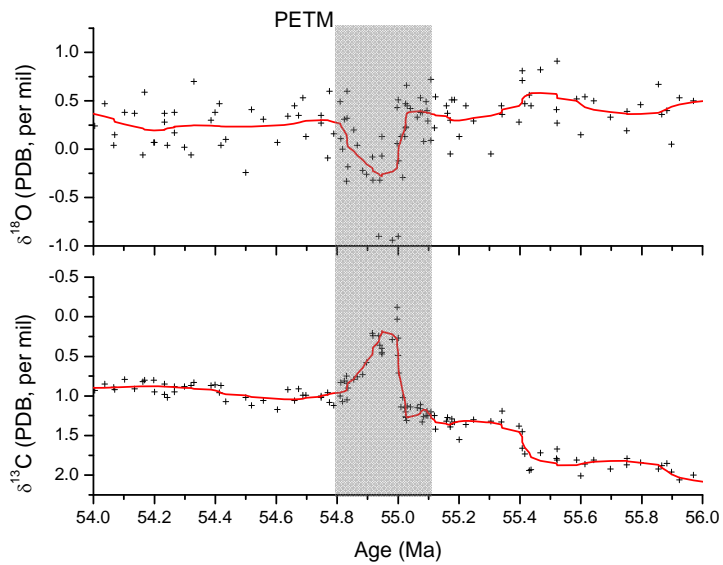


Fig.1.1. Composite marine oxygen and carbon isotopes reveal the Paleocene – Eocene thermal maximum (PETM) event occurred around ~ 55 Ma (Zachos et al., 2001). Negative excursion of oxygen isotope shows rapid global warming and $\sim 1\%$ $\delta^{13}\text{C}$ shift indicates light carbon injection into the ocean/atmosphere.

Archaea, methanotrophic archaea and their lipids

Archaea are one of the three domains of life on Earth. *Crenarchaeota* and *Euryarchaeota* are two major phyla of archaea. *Crenarchaeota* inhabit not only extreme environments like sulfidic, hot, salty or anoxic waters, but also widespread in other locations such as lakes, soils, open ocean and sediments (DeLong, 1992; Fuhrman et al., 1992; Jiang et al., 2008). The non-thermophilic crenarchaeota may account for one third of the planktonic prokaryotes in the open ocean (Karner et al., 2001). Mounting evidence shows that many of them are ammonia oxidizers (Francis et al., 2005; Konneke et al., 2005). Euryarchaeota, on the other hand, include important groups that mediate methane production (methanogens), as well as the anaerobic oxidation of methane (ANME groups). Microbial phylogeny and biogeochemistry evidence show that the methane oxidizers work in syntrophy with sulfate reducing bacteria to anaerobically oxidize methane (AOM) (Bioetius et al., 2000; Hinrichs et al., 1999; Hoehler et al., 1994) and the chemical reaction can be expressed as:



Geochemical investigations show that the AOM process is responsible for the consumption of 90% of the CH₄ produced in anoxic marine environment (Barnes and Goldberg, 1976; Reeburgh, 1976), which implies a close linkage between methane release and the AOM microbial community.

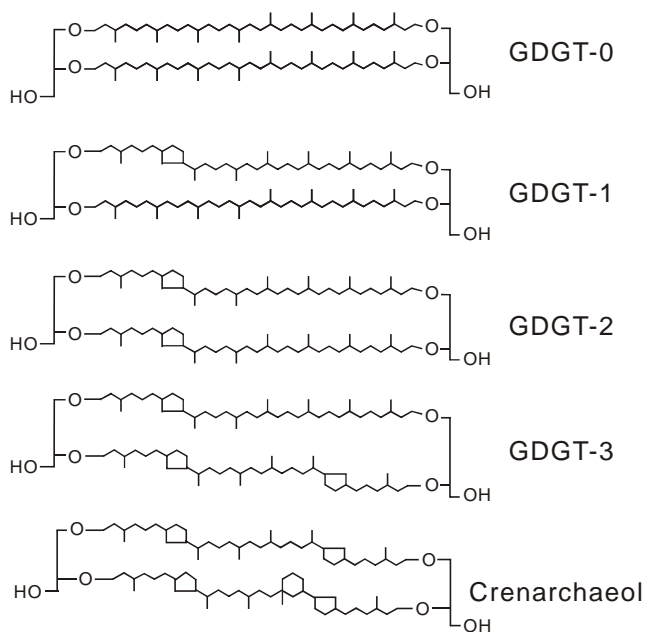


Fig. 1.2. Basic structures of five common GDGTs: GDGT-0, GDGT-1, GDGT-2, GDGT-3 and crenarchaeol. Crenarchaeol also has an isomer structure.

Archaea also have distinct lipids. Glycerol dialkyl glycerol tetraethers (GDGTs) are the core lipids of crenarchaeota (Koga et al., 1993). Euryarchaeota, on the other hand, are commonly characterized by isoprenoidal diethers such as archaeol and sn-2-hydroxyarchaeol (Hinrichs et al., 1999; Koga et al., 1998). However, some euryarchaeota such as ANME-1 also contain tetraethers as their core lipids (Blumenberg et al., 2004; Hinrichs et al., 1999). In particular, Blumenberg et al. (2004) observed a close relationship between ANME-1 group and cyclized GDGTs.

Five structures of archaeal GDGTs are commonly known (Fig. 1.2). Structures with zero, one, two or three cyclopentane rings are named GDGT-0, -1, -2 or -3, respectively. The structure with four cyclopentane rings and a cyclohexane ring is named as crenarchaeol and thought to be exclusively synthesized by crenarchaeota (e.g., Schouten et al., 2002). These molecules have specific biosynthesis origin and are quite stable and resistant to oxidation or degradation in geological formations (Brocks and Pearson, 2005). Therefore, GDGTs preserved in sediments could serve as molecular fossils archiving abundant paleo-biology, ecology and environmental information (Brocks and Pearson, 2005).

In this study we are developing a “methane index” that utilize the lipid biomarkers from methane oxidation reactions to evaluate the destabilization of gas hydrates in the Gulf of Mexico.

Chapter 2

Literature Review

GDGT Distribution in Normal Marine Environments

Schouten et al. (2000) first reported ubiquitous occurrence of isoprenoid GDGTs in marine environment, which is evidence of abundant non-hyperthermophilic archaea in seawater. The development of high performance liquid chromatography – atmospheric pressure chemical ionization – mass spectrometry (HPLC-APCI-MS) technique enabled rapid and precise measurement of intact tetraether archaeal lipids (Hopmans et al., 2000). This new technology facilitated GDGT studies in a number of environments like the open ocean (e.g., Turich et al., 2007), methane-rich water column (e.g., Wakeham et al., 2003), gas hydrate-rich deep-sea sediments (e.g., Pancost et al., 2001; Pi et al., 2009), terrestrial hot springs (e.g., Pearson et al., 2004; Pearson et al., 2008; Zhang et al., 2006), lake settings (e.g., Sinnighe Damste et al., 2009), and soils (e.g., Weijers et al., 2007).

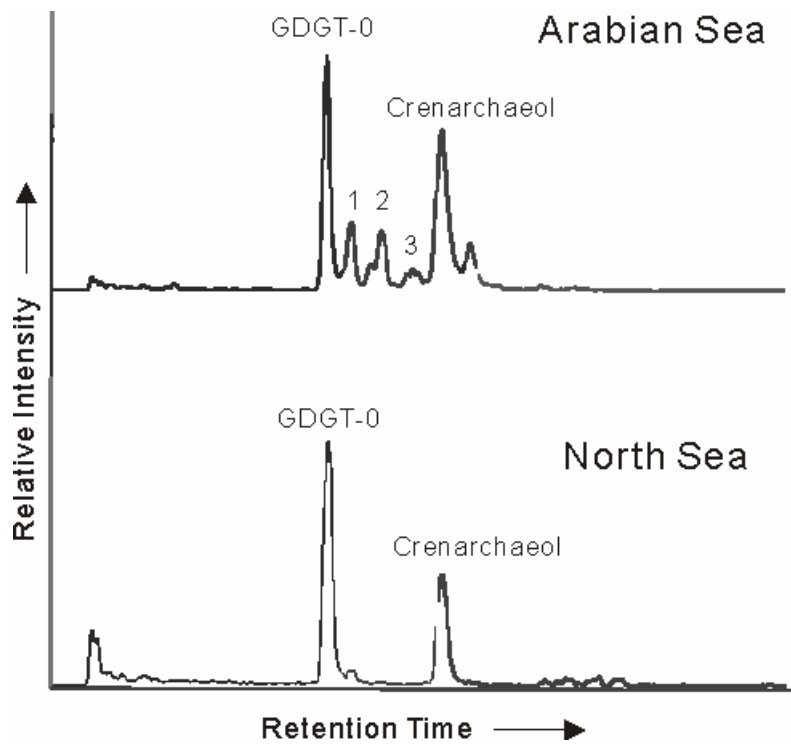


Fig. 2.1. HPLC/MS base peak chromatograms of surface sediment from the Arabian Sea and North Sea (Schouten et al., 2000; Schouten et al., 2002).

An intriguing finding of the GDGT distribution patterns in marine environment is that samples collected from cold areas like the North Sea (Fig. 2.1) consist almost completely of GDGT-0 and crenarchaeol. However, for samples collected from warmer areas such as the Arabian Sea (Fig. 2.1), they showed higher amount of additional structures with cyclized rings like GDGT-1, 2 and 3 (Schouten et al., 2000; Schouten et al., 2002). This is in accordance with what is observed in the (hyper)thermophilic genetic relatives of marine crenarchaeota, i.e. the weighted average number of cyclopentane rings in GDGTs substantially increases with growth temperature. Shouten et al. (2002) interpreted this as physiological adaptation of the archaea to temperature via biological synthesis of cyclopentane rings in the membrane lipids.

To quantify the GDGT distributions and express the control of temperature, Shouten et al. (2002) defined a TEX_{86} (TetraEther index of tetraethers consisting of 86 carbon atoms) index as the following:

$$TEX_{86} = \frac{(GDGT - 2) + (GDGT - 3) + (Cren - Isomer)}{(GDGT - 1) + (GDGT - 2) + (GDGT - 3) + (Cren - Isomer)}. \quad (2.1)$$

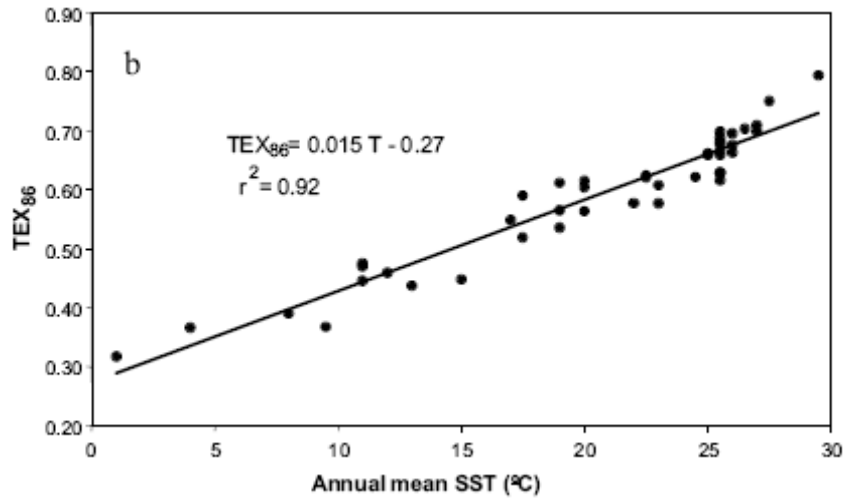


Fig. 2.2. Relationship between the TEX₈₆ index and annual mean SST from 40 surface sediments collected from 15 locations worldwide. From Schouten et al., (2002).

Schouten et al. (2002) collected 40 surface sediments from 15 different worldwide locations and plot the TEX_{86} vs. sea surface temperature (SST) in Fig. 2.2 which clearly exhibit a linear relationship between the two variables and the linear regression gives the function:

$$TEX_{86} = 0.015T - 0.27, \quad (2.2)$$

Where T is the sea surface temperature (SST).

To further validate the temperature control on archaeal lipid distributions, a subsequent mesocosm incubation study was performed (Wuchter et al., 2004). Marine crenarchaeota were incubated at the temperatures ranging from 5 to 35 °C and salinity of 27 and 35‰ for three months. With increasing temperature, an increase in the number of cyclopentane moieties was observed (Fig. 2.3.). Different salinities did not show any effect on the GDGT distribution (Wuchter et al., 2004). This study confirmed the correlation between incubation temperature and the TEX_{86} index (Fig. 2.4).

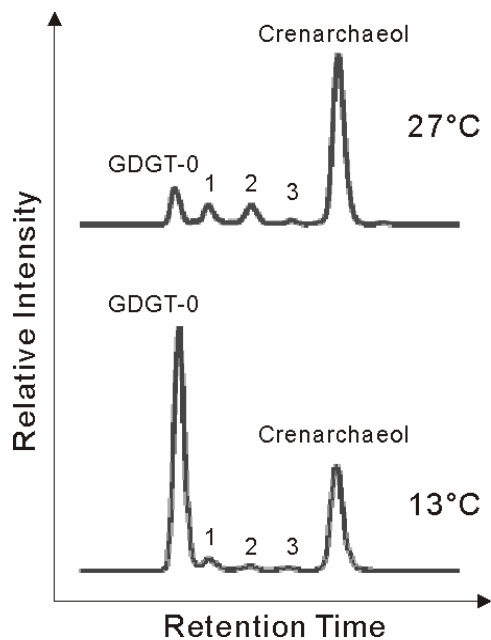


Fig. 2.3. Partial HPLC-APCI/MS base peak chromatograms of particulate organic matter derived from the mesocosm tank experiments after incubation for three months at 27°C and 13°C, respectively. Modified from Wuchters et al., (2004).

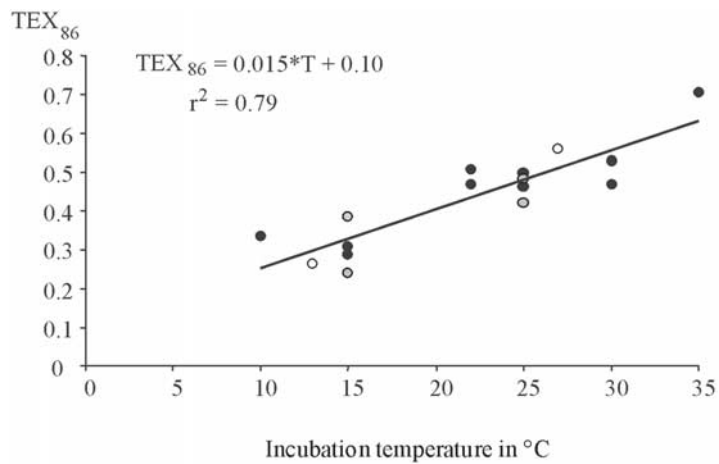


Fig. 2.4. Correlation of the incubation series. Black dots represent TEX₈₆ values from incubation at 27‰ salinity, and gray dots represent TEX₈₆ values from incubation at 35‰ salinity. Open dots represent TEX₈₆ values from the initial mesocosm water. From Wuchter et al., (2004).

The TEX_{86} index appears to be robust diagenetically. Since archaeal lipid biomarkers for TEX_{86} calculation have been found in sediments spanning the last 100 million years, they complement other organic SST proxy such as U_k^{37} , and can go back much further in time. Moreover, TEX_{86} is capable of recording higher temperatures ($> 30\text{ }^\circ\text{C}$), at which the U_k^{37} proxy from algae alkenones would be muted (Eglinton and Eglinton, 2008). Therefore, this novel SST proxy has been used intensively in recent paleoclimate studies, revealing the high SST in middle Cretaceous low latitudes (Forster et al., 2007; Schouten et al., 2003), global cooling at the Eocene-Oligocene boundary (Liu et al., 2009), and late Quaternary SST fluctuations in the Arabian Sea (Huguet et al., 2006). Besides, similar relationship between temperature and GDGT distribution was also found in lacustrine environments, indicating the potential of TEX_{86} in lake temperature reconstruction (Powers et al., 2004). Another notable progress is that Kim et al. (2008) recently improved the calibration for determine the TEX_{86} against SST by a more complete survey of global ocean core-top sediments. The linear relationship has been updated as

$$T = -10.78 + 56.2 * TEX_{86} \quad r^2 = 0.935, n = 223 \quad (2.3)$$

The temperature, however, is not the only factor controls the changes in membrane structure of archaea. Other environmental or physiological/genetic changes may also make contributions. Specifically, in the marine environment where free methane and/or cold seep of gas hydrates abundantly occur, their GDGT profiles can hardly be explained by temperature controls. Instead, microbial community shift could most likely be the

case.

GDGT Distribution in Gas Hydrate Impacted Environments

In methane-rich marine environment like the Mediterranean cold seeps (Fig. 2.5e) (Pancost et al., 2001), Gulf of Cadiz authigenic carbonates (Stadnitskaia et al., 2008), Gulf of Mexico hydrate impacted sites (Fig. 2.5f) (Pi et al., 2009), and Black Sea water column (Wakeham et al., 2004; Wakeham et al., 2003), analysis of archaeal lipids revealed that the GDGT distribution is distinct from that in normal marine water column or sediments. Namely, in methane-rich or hydrate-impacted environments, the GDGT profiles are characterized by pronounced increases in the relative abundance of cyclized GDGTs like GDGT-1, GDGT-2 and GDGT-3 (Fig. 2.5, e, f). Although warmer temperature would also increase GDGTs with cyclopentane rings (Fig. 2.5, c, d), those increases observed in hydrate impacted environments are greater than the archaeal temperature responses.

Molecular microbiology and phylogeny studies indicate that in the gas hydrate impacted and/or methane released marine environments, the abundance of methanotrophic euryarchaeota, the ANME group, increases dramatically (e.g., Pi et al., 2009). Those archaea have been assigned to three phylogenetic clusters, ANME-1, ANME-2 and ANME-3. Although the pure culture of neither of the three groups is available at present, *in situ* environmental studies showed that the predominated ANME-1 archaea yield internally cyclized GDGTs, with preferential synthesis of GDGT-1 and GDGT-2, and to some extent GDGT-3 (Blumenberg et al., 2004).

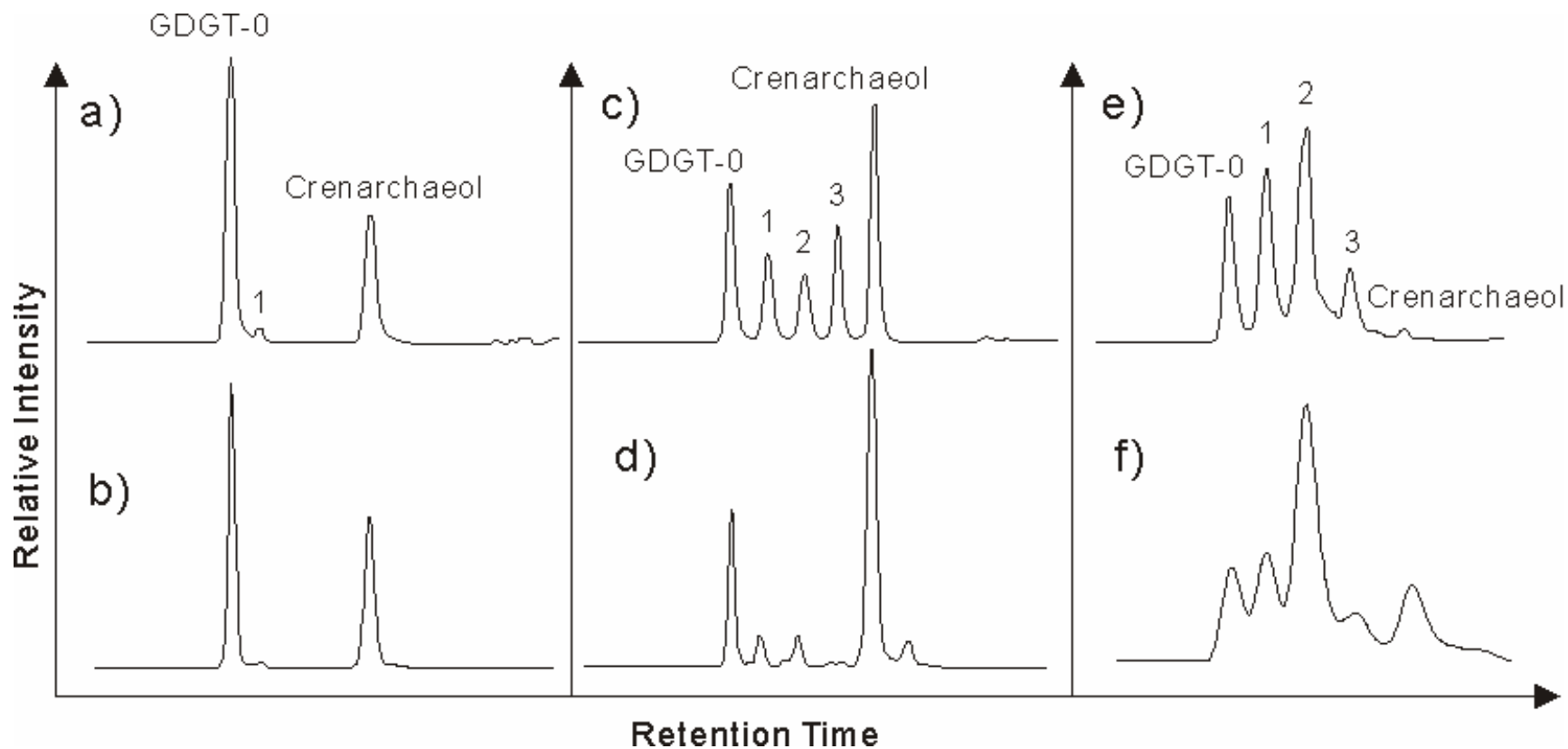


Fig. 2.5. HPLC-APCI/MS peak chromatogram showing the GDGT distribution in different environments. Left panel: cold marine environment. a) Skagerrak (North Sea) (Schouten et al., 2000), b) Halley Bay (Antarctica) (Schouten et al., 2002). Middle panel: archaeal lipids from warm environments. c) cultured crenarchaeota “*Candidatus Nitrosopumilus maritimus*” incubated at 28 °C for

three months (Schouten et al., 2008), d) surface sediments from Arabian Sea (Schouten et al., 2002). Right panel: gas hydrate impacted environment. e) Mediterranean cold seeps (Pancost et al., 2001), f) Gulf of Mexico gas hydrate site MC 118 (Pi et al., 2009).

Based on the discussion above, we suggest that in the gas hydrate impacted marine environments where methane releases abundantly occur, the closely associated ANME methanotrophic archaea would contribute significantly to the GDGT pool with internally cyclized GDGTs, separating the GDGT profiles in those environments from these in the normal marine sediments. Since GDGTs preserved in sediments could serve as molecular fossil, appropriate utilization of the GDGT signatures could help us to identify gas hydrate reservoir destabilization in Earth's geological past.

Chapter 3

Gas Hydrate Impacted Environments in the Gulf of Mexico: A Natural Laboratory for Methane Index Studies

Materials

The Gulf of Mexico (GOM) represents a unique system for biogeochemistry and geomicrobiology studies of gas hydrates because of the wide occurrence of cold seeps, free gas venting, diverse microbial communities and authigenic carbonate platforms within the ~ 1.6 million km² gulf basin (Fig. 3.1) (Sassen et al., 2004; Zhang and Lanoil, 2004). Previous studies of lipids, isotope and molecular biology showed the consortia of methanotrophic archaea and sulfate reducing bacteria mediated AOM in the GOM (Pancost et al., 2005; Zhang et al., 2003; Zhang et al., 2002). Besides, the gas hydrates in GOM are predominantly Structure II, whereas gas hydrates at most other locations are Structure I. The difference is primarily due to the source of the hydrocarbons for the gas hydrates: Structure II gas hydrates are usually fueled by thermogenic methane plus C₂ – C₅ hydrocarbons from crude oil formations. Structure I are considered biogenic with the methane produced by methanogenic archaea (Zhang and Lanoil, 2004).

In this study we utilized core sediment samples recovered from Mississippi Canyon Block 118 (MC 118), located on the northeastern gulf slope. MC 118 gas hydrate site was discovered by the Johnson Sea-Link research submersible in 2002. Free gas (C₁-C₅ hydrocarbons and minor CO₂) vents from the sea floor to the water column at ~ 890 m depth where temperature is ~ 5.7 °C. This site is characterized by crater-like depressions

and mounds of authigenic carbonate rocks over an area of $\sim 1 \text{ km}^2$. The carbonates are the results of microbial oxidation of hydrocarbons (primarily CH_4), because the AOM process as expressed in reaction 1.1, 1.2 and 1.3 would generate bicarbonates, which will increase the pH in the ambient environment and favor carbonate precipitation. Abundant chemosynthetic communities like microbial mats (*Beggiatoa*), tube worms, mussels, and bivalves have been developed around the gas vents (Sassen et al., 2006). A preliminary study by Sassen et al. (2006) showed that methane (94.4 – 96.5%) is the main component of the venting gas. Isotopic properties of CH_4 ($\delta^{13}\text{C} = -45.7\text{‰}$, $\delta\text{D} = -163\text{‰}$) are consistent with a deep source that also generated crude oil. Ethane, propane, butanes and pentanes are the minor components. The $\delta^{13}\text{C}$ of CO_2 from vent gas is strongly enriched in ^{13}C (as much as $+25\text{‰}$), as typical of a deeply buried source (Sassen et al., 2006).

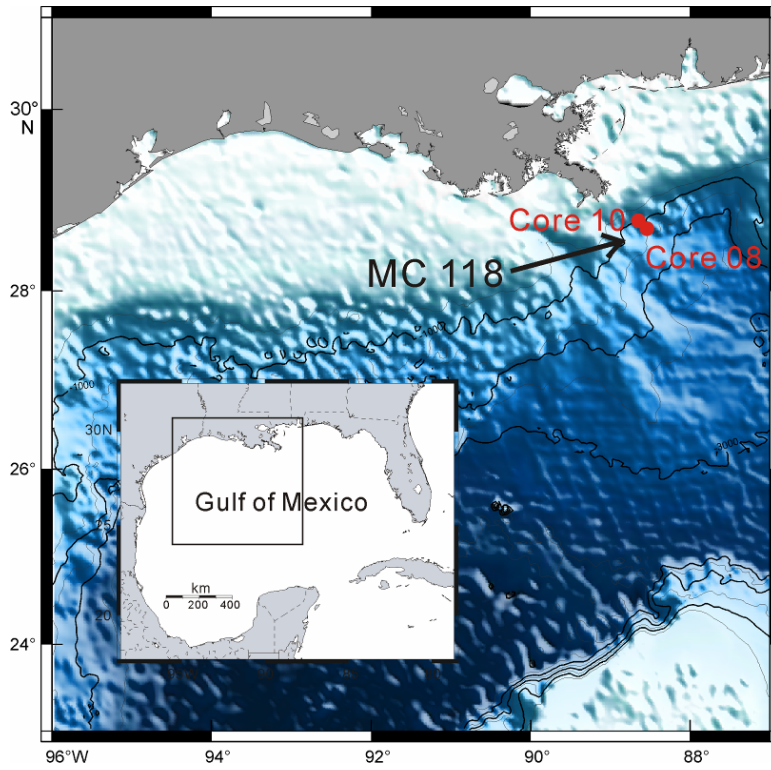


Fig. 3.1. Map showing the location of Mississippi Canyon Block 118 (MC 118) in the north Gulf of Mexico and northeast of the Mississippi Canyon. Core 08 and Core 10 are two sediment cores used in this study.

In April 2008, 26 gravity cores were collected from MC 118 during a cruise by the R/V Pilican. We obtained two sediment cores, Core 08 and Core 10. Core 08 is about 7 m in length and Core 10 ~ 1.3 m in length. About 50 grams of sub-samples were taken from the core, yielding 16 samples for Core 08, and 14 samples for Core 10. Core 08 is located off the hydrate mound; and gas hydrate impact is minimal (Fig. 3.2). Core 10 is on the southwest side of the hydrate mound, which is thought to be impacted by gas hydrate (Fig. 3.2). The lithology is similar to previous samples collected from MC 118 (Pi et al., 2009). In general, all cores were dominated by mud (particle size < 0.063 mm) and contained less than 10% sand (particle size ranging from 2-0.063 mm) in most intervals (Pi et al., 2009). Samples were stored in a -20 °C freezer onboard and -80 °C in the laboratory until analysis. Some other basic information about the two cores is listed in Table 3.1.

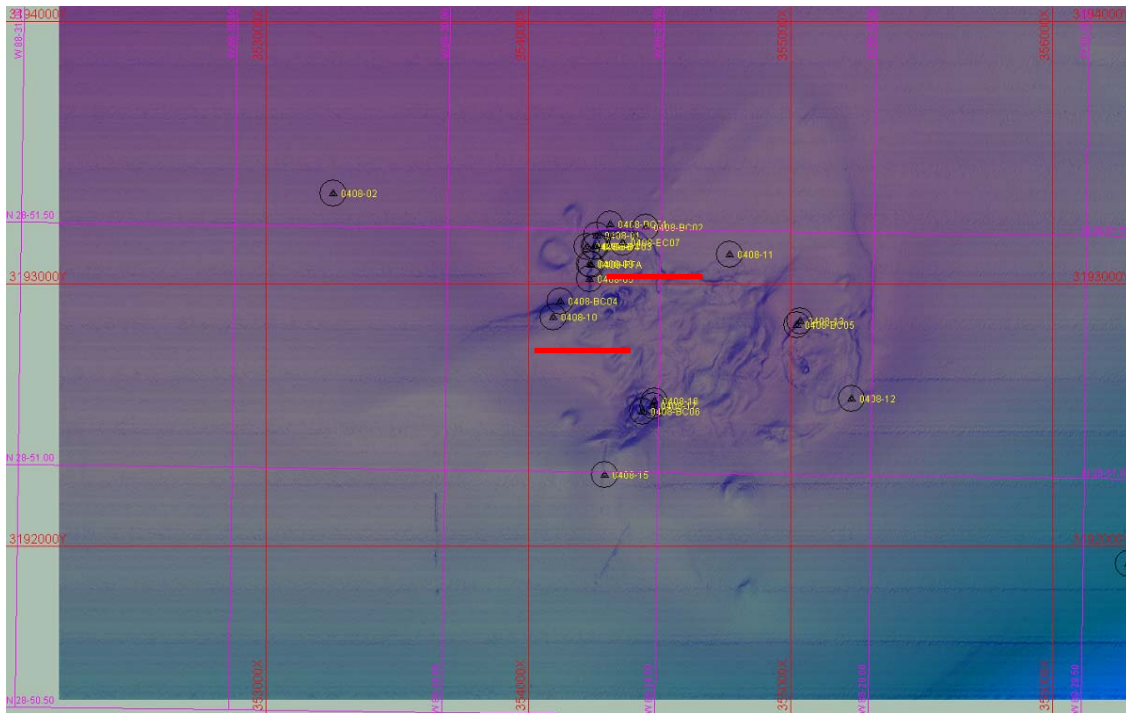


Fig. 3.2. Seafloor imagery of MC 118 showing the sampling site during the April 2008 R/V Pelican cruise. Core 08 and Core 10 are highlighted with underlying red lines. Core 08 is located off the gas hydrate mound whereas Core 10 is on the southeast corner of the hydrate mound.

Tab. 3.1. Sampling information for Core 08 and Core 10 in MC 118 during the 2008 R/V

Pelican cruise.

Core	Sampling Date	Latitude (°)	Longitude (°)	Water Depth (m)
08	4/24/2008	28 50 42.7943	88 27 53.3108	971
10	4/28/2008	28 51 19.0349	88 29 44.9651	878

Pore Water Chemistry

The frozen samples were thawed to room temperature. About 20 grams of wet samples were centrifuged at 3000 rpm for 20 minutes for the collection of the pore water. The pore water samples were immediately diluted by anoxic water for measurements of sulfate and hydrogen sulfide using Hach Kits according to the manufacturer's instructions (Hach Company, Loveland, CO).

Stable Isotopes of Carbonates

After extraction for porewater, solid samples were freeze-dried and ~ 2 g of sample were used for analysis of stable carbon and oxygen isotopes. Samples were subject to $\delta^{18}\text{O}$ and $\delta^{13}\text{C}$ measurements on a MAT 252 isotope ratio mass spectrometer in the State Key Laboratory of Marine Geology at Tongji University. Standard isotopic corrections were made and the oxygen and carbon isotopes were reported relative to the PDB scale. The precision (1σ) is ≤ 0.1 ‰ for $\delta^{13}\text{C}$ and ≤ 0.2 ‰ for $\delta^{18}\text{O}$.

Lipid Analysis

About 5 g lyophilized samples were used for lipid analysis. Total lipid extraction was performed following Zhang et al. (2006). We used a single-phase organic solvent system comprised of chloroform, methanol, and aqueous 50-mM phosphate buffer (pH = 7.4) in the ratio of 1:1:0.8 (v:v:v). After about 12 hours, equal volumes of chloroform and nano-pure water were added, forming a two phase system. The organic phase was collected and reduced in volume under pure N_2 gas.

Total lipids were transesterified in 2 ml of methanol and hydrochloric acid (95:5, v/v)

in a heating block at 70 °C for 2 hours to hydrolyze polar side-chains of GDGTs. After cooling to room temperature, 1 ml of solvent-extracted nano-pure water and 2 ml of dichloromethane (DCM) were added. The transesterified lipids were passed through a C-18 solid phase extraction (SPE) column using different solvents. Four fractions were eluted: Polar I, Polar II, GDGT and neutral lipids. The GDGT fraction was eluted with 1:3 ethyl acetate:hexane and then evaporated under N₂ gas stream. Extracted GDGT fraction was separated into two aliquots, one aliquot was send out for LC-MS analysis and the other one was stored for ether cleavage experiments and compound specific isotope analysis.

HPLC-MS analysis was performed at the University of Bremen in Bremen, Germany. Samples were dissolved in 200 µl of hexane/isopropanol (99:1, v/v) for injection. Analysis of GDGT core lipids followed a slightly modified method developed in Hopmans et al. (2000). Separation of GDGTs was achieved on an Econosphere NH₂ column (250 * 4.6 mm, Alltech, Germany) heated to 30 °C in a Thermo Finnigan Surveyor HPLC system. The following gradient was used at 1 ml/min flow rate: hold isocratically at 99:1 hexane/isopropanol (v/v) for 5 min, then ramping to 98.2:1.8 hexane/isopropanol (v/v) at 45 min, followed by flushing with 95:5 hexane/isopropanol (v/v) for 10 min and equilibrating with 99:1 hexane/isopropanol (v/v) for 10 min to prepare the system for the next injection. Mass spectrometric identification and quantification was applied on a Thermo Finnigan LCQ Deca XP Plus ion trap mass spectrometer coupled to the HPLC by an atmospheric pressure chemical ionization (APCI)

interface. APCI settings were as follows: capillary temperature 200°C, source heater temperature 400°C, sheath gas flow 30 arbitrary units, source current 5 μ A, while other parameters were optimized by manual tuning during infusion of a hydrolyzed commercially available intact GDGT standard (Matreya, USA). Samples were analyzed using selected ion scans, from 0 to 5.5 min at m/z 600-700 and from 5.5 to 45 min at m/z 1200-1500. Quantification of core lipids and calculation of relative ring distribution were generated from mass chromatograms of the M⁺ ions.

GDGT Cleavage and Compound Specific Isotope Analysis

Stable carbon isotopes can be helpful to trace the carbon flow from substrates to the biomass of microorganisms. Since compound specific isotope analysis gives us the information of specific organic compound that is utilized by the microorganisms, it's becoming a powerful tool in biogeochemical studies. Methane almost always has very negative $\delta^{13}\text{C}$ values; therefore, it would be easy to trace the carbon flow pathways from methane to microbial biomass.

Determination of the carbon isotopes of GDGTs would be able to reveal what the carbon source is (methane or non-methane). However, because of the large molecular weight of GDGTs, they cannot be tested on Gas Chromatography – Isotope Ratio Mass Spectrometer (GC-IRMS). One approach to solve this problem is to do the ether cleavage through HI treatment and the reduction of resulting iodides by using AlLiH_4 . The GDGTs will be cleaved into phytane and biphytane which have much smaller molecular weights. Detailed treatment is the following:

- 1) Add approximately 2 ml 57% HI to the nitrogen-dried GDGT fraction in the 1st test tube. Then tightly wrap the vial in aluminum foil and heat at 110°C for about 4 hours.
- 2) Once the vials are cooled down, add 2 mL 10% NaCl.
- 3) Extract with 4 mL n-hexane (repeated 3 times) and transfer the extraction into the 2nd test tube.
- 4) Add Na₂SO₄ and set overnight.
- 5) Transfer the sample from the Na₂SO₄-contained test tube into the 3rd test tube, and reduce the sample volume to about 1 ml under N₂. Then transfer to the React-vial.
- 6) Insert the nitrogen needle and a syringe through the septa. Keep the nitrogen stream for about 1 minute to pull out the oxygen. Remove the nitrogen needle and syringe.
- 7) Carefully add 2 mL LiAlH₄ into each sample using the solvent rinsed syringe and needle. Then heat for 2 hours at 70 degree centigrade.
- 8) Remove vials from the heating block and allow samples to cool down completely.
- 9) Quench the reaction with 0.5 mL ethyl acetate (Insert the needle into the septum and add ethyl acetate as slowly as possible. If the reaction does not stop when all 0.5 ml ethyl acetate is added, more ethyl acetate solvent is needed).
- 10) Wait a couple of minutes to cool it down. Extract 4 times using ethyl acetate and sit overnight on Na₂SO₄.
- 11) Finally dry samples under N₂.

Once dried, the samples were transferred to a GC-IRMS for compound identification and compound-specific isotope analysis.

Chapter 4

Results and Discussion

Pore Water Chemistry and Carbonate Isotopes

. In Core 08, the sulfate concentration in pore water is high (15.6-36.5, Table 4.1), whereas sulfide is close to 0 in most of the samples (Fig. 4.1A). Three depth intervals have detectable sulfide concentrations: 91 cm with H₂S of 14.7 μM, 501 cm with H₂S of 14.7 μM, and 701 cm with H₂S of 29.4 μM (Table 4.1). In Core 10, sulfate decreased with depth and hydrogen sulfide increased with depth (Fig. 4.1B). This is similar to a typical profile for AOM, indicating significant microbially mediated methane oxidation, especially in the deeper part of Core 10 (Fig. 4.1B).

The δ¹³C of bulk carbonates varied from -0.37 to 1.30 ‰ in Core 8 and varied from -28.08 to -1.17‰ in Core 10. The δ¹⁸O of bulk carbonates varied from -4.84 to 0.85 ‰ in Core 8 and -3.06 to 4.08 ‰ in Core 10. Previous studies show that in methane-rich environments both foraminifera carbonate shells (e.g., Kennett et al., 2000) and authigenic carbonates (e.g., Stadnitskaia et al., 2008) would have negative δ¹³C values. Stadnitskaia et al. (2008) found that in the Gulf of Cadiz where the gas hydrate is thermogenic, the AOM associated carbonates have their δ¹³C values between -20 and -27‰. In Gulf of Mexico we identified the hydrate-impacted samples having δ¹³C values as low as -28.08‰. If we assume a simple two end member model for the C source of carbonate: CH₄ which has the δ¹³C = -46‰ (Sassen et al., 2006) and the bicarbonates in the pore water (δ¹³C = ca. 0 ‰), then we have

$$-46 \times x + 0 \times (1 - x) = -28.08$$

$$x \approx 0.61$$

Thus, the maximum contribution of oxidation of methane to the carbonate carbon pool is about 61% (Formolo et al., 2004).

Table 4.1. Pore water chemistry and stable carbon and oxygen isotope data for Core 08 and Core 10.

Core 08				
Depth (cm)	Sulfate (mM)	Sulfide (μM)	$\delta^{13}\text{C}$ (‰, PDB)	$\delta^{18}\text{O}$ (‰, PDB)
6	35.4	0	1.07	0.24
21	35.9	0	1.10	0.29
31	35.4	0	1.23	0.28
41	34.9	0	1.02	0.23
51	29.2	0	0.90	0.51
61	29.2	0	0.70	0.25
71	36.5	0	0.92	0.80
81	35.4	0	0.81	0.85
91	32.3	14.7	0.47	0.11
101	34.9	0	0.72	-1.24
201	33.3	0	0.76	-0.84
301	32.8	0	1.30	0.27
401	30.2	0	-0.13	-4.57
501	21.4	14.7	-0.37	-4.84
601	15.6	0	0.20	-3.20
701	20.8	29.4	0.15	-3.51

Core 10				
Depth (cm)	Sulfate (mM)	Sulfide (μM)	$\delta^{13}\text{C}$ (‰, PDB)	$\delta^{18}\text{O}$ (‰, PDB)
1	30.2	0	-1.17	0.58
11	32.8	14.7	-6.69	1.24
21	27.1	14.7	-14.75	1.55
31	29.7	0	-27.32	4.08
41	26.6	0	-15.02	-0.11
51	25	14.7	-19.53	1.29
61	16.7	44.1	-8.78	-1.81
71	13.5	382.4	-10.38	-1.33
81	13.5	176.5	-8.31	-1.37
91	11.5	88.2	-10.72	-1.22
101	9.9	14.7	-23.90	2.39
111	5.2	73.5	-6.89	-3.06
121	4.7	8.8	-28.08	3.64
130	0	161.8	-12.16	-0.91

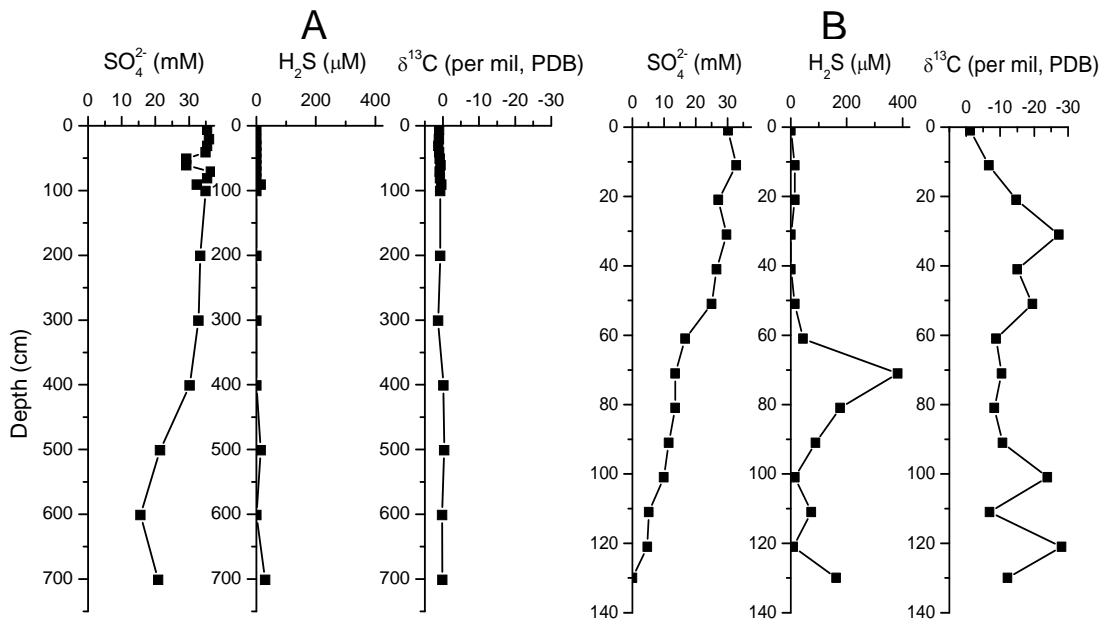


Fig. 4.1. Vertical profiles of sulfate, sulfide, and stable carbon isotope for Core 08 (A) and Core 10 (B) in MC 118, Gulf of Mexico. Core 08 shows high sulfate, low sulfide concentrations with relatively higher $\delta^{13}\text{C}$ values, which indicate that gas hydrate impact is limited in this sediment core. Core 10 shows decreasing sulfate and increasing sulfide trend with depth, accompanied by more negative $\delta^{13}\text{C}$ values than in Core 08.

The above observations point to the fact that Core 08 is likely a normal marine sedimentation with limited influence of gas hydrates, whereas Core 10 is a hydrate-impacted environment with active AOM occurring within the deeper depth of this core.

Another intriguing finding is that in Core 10, carbonate $\delta^{13}\text{C}$ is reversely correlated with $\delta^{18}\text{O}$ (Fig. 4.2). Methane-contributed carbon would be ^{13}C depleted. Meanwhile, water released from the decomposition of gas hydrate would be ^{18}O enriched (Stadnitskaia et al., 2008).

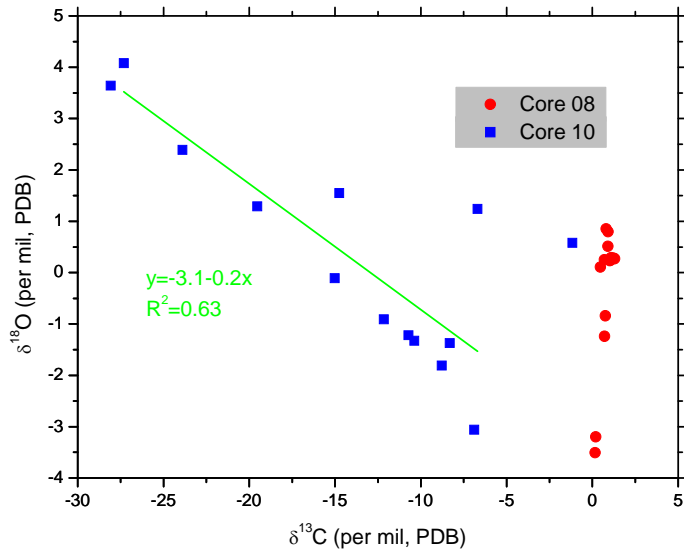


Fig. 4.2. Correlations between carbonate $\delta^{18}\text{O}$ and $\delta^{13}\text{C}$ for Core 08 and Core 10. A reverse correlation between $\delta^{18}\text{O}$ and $\delta^{13}\text{C}$ was found in Core 10 as indicated by a linear regression. The regression function is $y = -3.1 - 0.2x$ with the r^2 equals 0.63.

To sum up, all of the pore water chemistry and carbonate stable isotope evidence implied that in our study, Core 08 probably is normal marine sedimentation with limited gas hydrate impact, whereas Core 10 shows significant AOM associated with hydrates and free methane. Therefore, those two sediment cores could serve as contrasting cases. Archaeal lipid studies in those two different environments would show how the lipids respond to presence/absence of gas hydrates (see below).

Archaeal Lipids

Archaeal tetraether lipids, the GDGTs, have been identified in all samples. In Core 08, crenarchaeol is the predominant GDGT, ranging from 49.23 to 57.23 % (Table 4.2). This result is consistent with archaeal lipids from normal marine environment. In contrast, in Core 10 where the environment has been impacted by gas hydrates, deeper depths in particular, the relative abundances of GDGT-1, GDGT-2 and GDGT-3 increase dramatically (Table 4.2). These results are similar to what have been reported for the Black Sea (Wakeham et al., 2004; Wakeham et al., 2003), the Mediterranean (Bouloubassi et al., 2006; Pancost et al., 2001), the Gulf of Cadiz (Stadnitskaia et al., 2008), and an earlier study at the Gulf of Mexico (Pi et al., 2009).

Table 4.2. Relative abundance of the GDGTs (%) in Core 08 and Core 10, MC 118, Gulf of Mexico.

Core 08						
Depth (cm)	GDGT-0	GDGT-1	GDGT-2	GDGT-3	Crenarchaeol	Cren Isomer
6	24.12	6.54	7.67	1.55	55.62	4.49
21	22.35	6.62	7.93	1.52	56.55	5.03
31	25.61	7.32	9.52	1.73	51.44	4.38
41	23.87	6.55	8.33	1.44	55.55	4.26
51	23.45	7.29	8.48	1.35	54.87	4.57
61	24.01	7.51	7.58	1.86	54.84	4.20
71	27.11	8.44	8.46	1.53	50.81	3.65
81	24.66	7.73	8.04	1.48	53.71	4.38
91	26.58	6.53	8.72	1.85	52.14	4.18
101	27.81	8.32	8.50	1.66	50.01	3.71
201	27.48	7.41	8.38	1.46	51.17	4.09
301	29.39	7.59	8.21	1.51	49.23	4.07
401	27.28	7.59	8.72	1.29	50.02	5.09
501	24.36	7.08	9.51	1.30	52.73	5.01
601	25.42	7.49	8.81	1.40	51.47	5.42
701	21.82	6.93	8.15	1.25	57.23	4.63

Core 10						
Depth (cm)	GDGT-0	GDGT-1	GDGT-2	GDGT-3	Crenarchaeol	Cren Isomer
1	25.96	7.49	8.50	1.72	52.65	3.68
11	25.72	10.34	13.66	2.59	44.13	3.56
21	29.70	14.35	24.31	4.75	24.47	2.42
31	43.77	16.93	17.94	3.21	16.56	1.58
41	31.61	19.01	30.75	5.32	12.21	1.10
51	29.94	15.86	26.07	3.74	22.26	2.13
61	28.10	15.14	20.68	3.83	28.95	3.29
71	30.24	14.32	19.98	2.78	29.47	3.20
81	31.46	15.06	22.47	3.10	25.76	2.15
91	28.70	12.96	20.86	3.23	31.29	2.97
101	37.49	17.63	28.65	6.29	8.99	0.95
111	26.52	17.77	30.92	5.31	17.15	2.32
121	19.52	24.06	43.67	8.09	4.04	0.62
130	38.87	21.40	29.82	5.94	3.51	0.45

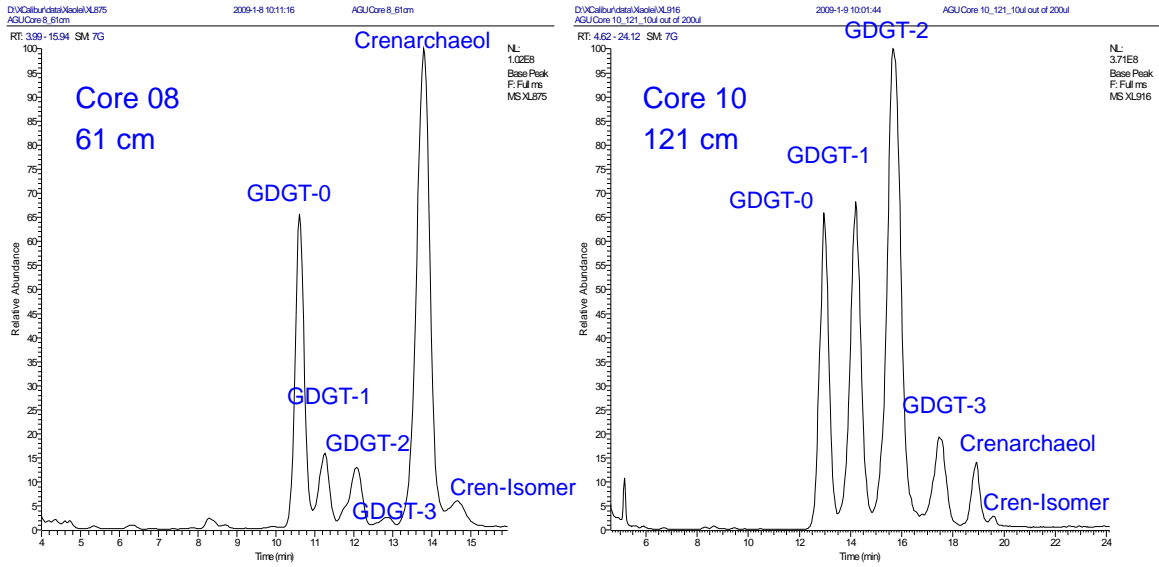


Fig. 4.3. HPLC/APCI-MS peak chromatogram of two typical samples: Left panel, Core 08, 61 cm; Right panel, Core 10, 121 cm. This figure reveals that the GDGT distribution in those two cores is quite different. Normal marine environment (Core 08) is dominated by crenarchaeol, whereas hydrate-impacted environment (Core 10) is characterized by significant enhancement of GDGT-1, GDGT-2 and GDGT-3.

The GDGT distribution in Core 08 and Core 10 is plotted in Fig. 4.4 against the sample depth. Again, crenarchaeol dominates in Core 08, but GDGT-1, GDGT-2 and GDGT-3 are enhanced along the vertical profile in Core 10. These phenomena cannot be explained by the temperature responses of crenarchaeota because the relative abundance of cyclized GDGTs abundance is out of the ranges of temperature responses. Instead, the most likely case is that archaeal groups other than planktonic crenarchaeota contributed to GDGT pool preserved in marine sediments. Because several lines of evidence point to profound AOM in Core 10, and methanotrophic ANME-1 archaea show strong preference of synthesizing cyclized GDGTs (Blumenberg et al., 2004; Pi et al., 2009), we propose that the presence of methanotrophic ANME-1 group euryarchaeota should be responsible for the GDGT distribution patterns that we have observed in Core 10.

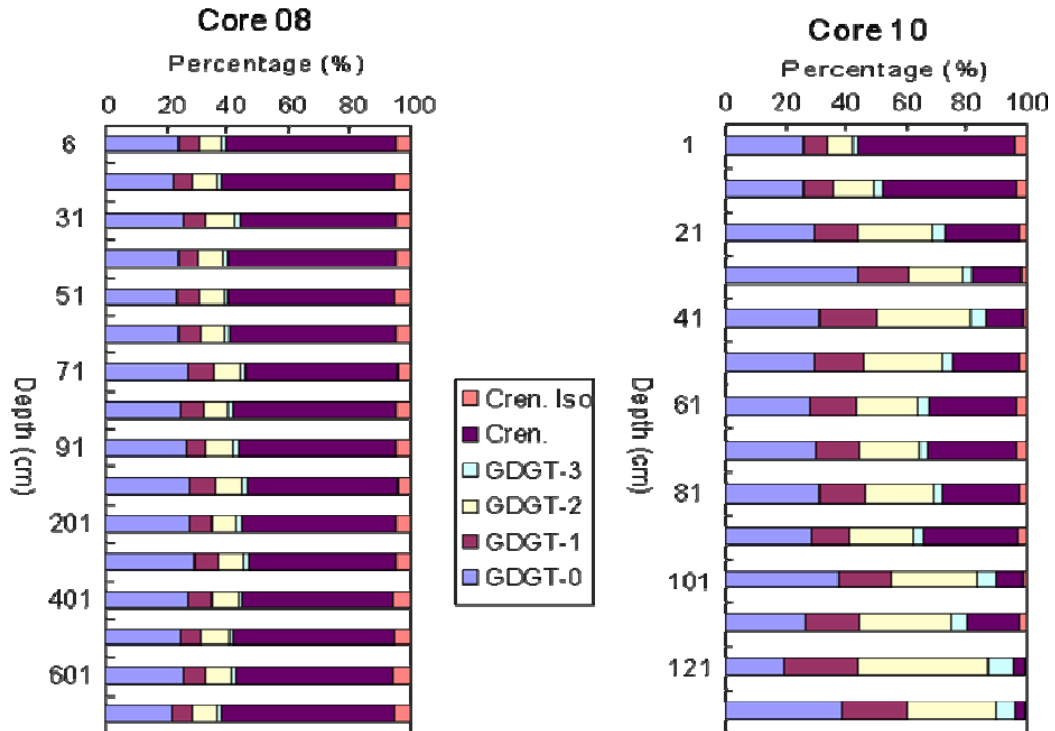


Fig. 4.4. Vertical distribution of GDGTs in Core 08 and Core 10, MC 118, Gulf of Mexico. Through the entire Core 08, crenarchaeol is the predominant GDGT with little variations in its relative abundance. Whereas in Core 10, GDGT-1, GDGT-2 and GDGT-3 show significant enhancement in the deeper depths.

Methane Index: Definition and Verification

In order to quantify the difference between planktonic crenarchaeota and methanotrophic euryarchaeota in the GDGT pool in either normal marine or hydrate impacted marine environment, we define a “Methane Index” as

$$MI = \frac{[GDGT - 1] + [GDGT - 2] + [GDGT - 3]}{[GDGT - 1] + [GDGT - 2] + [GDGT - 3] + [Crenarchaeol] + [Cren.Isomer]} \quad (4.1)$$

This definition is based on the fact that planktonic crenarchaeota preferentially synthesize crenarchaeol whereas methanotrophic euryarchaeota are likely to produce cyclized GDGTs, namely GDGT-1, GDGT-2 and GDGT-3. Methane index should have the range from 0 to 1: the bigger the number, the stronger impact that the ANME groups in a particular environment, indicating the occurrence of gas hydrate dissociation and/or free methane release; the smaller the number, the stronger planktonic crenarchaeota influence in the environment, characterizing the normal marine water column and sedimentation.

The depth dependent variation of MI is shown in Fig. 4.5, which reveals the same environmental conditions as pore water chemistry and carbonate isotopes did. Core 08 has fairly low MI (around 0.2) with little variations along the depth. However, Core 10 shows relatively high MI (maximum value close to 0.94) and an increasing trend with the increase in sample depth. Apparently, the MI provides more direct insights of the gas hydrate dissociation and AOM in the sediments than other existing proxies.

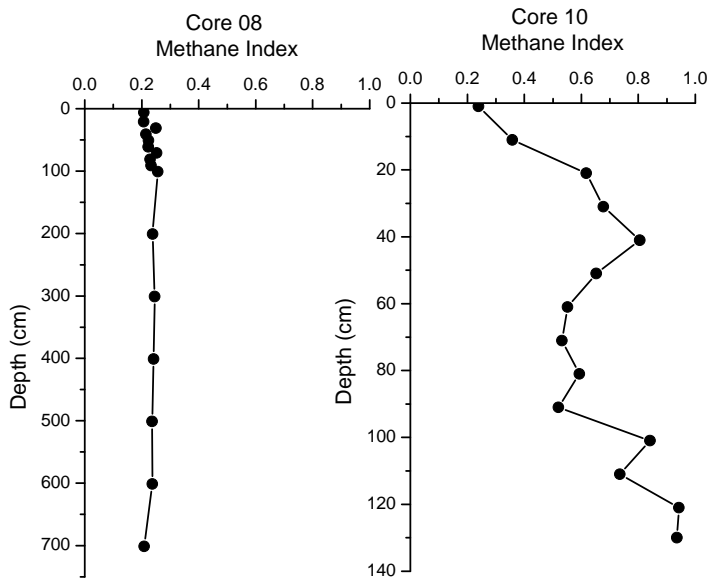


Fig. 4.5. Depth dependent methane index for Core 08 and Core 10, MC 118, Gulf of Mexico. Core 08 shows fairly low and stable MI values whereas Core 10 exhibits high and increasing trend of MI with the increase in sample depth.

Methane Index vs. Compound-specific carbon isotopes

To further validate this methane index, we did compound-specific $\delta^{13}\text{C}$ analysis for selected samples from Core 08 and Core 10. After HI reduction and ether cleavage, the tetraether was cleaved into biphytanes with their structures shown in Fig. 4.5. The $\delta^{13}\text{C}$ of the cleaved phytane and biphytanes are shown in Table 4.3.

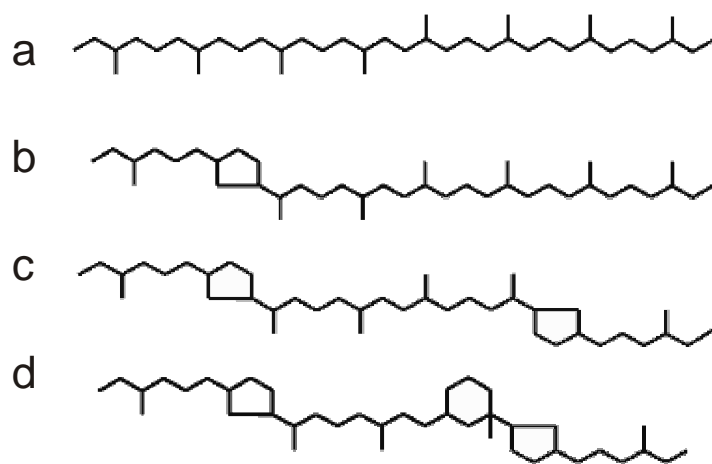


Fig. 4.6. Structures showing the biphytanes released from ether cleavage of GDGTs:
 biphytane a (acyclic), b (monocyclic), c (bicyclic) and d (tricyclic).

Table 4.3. Methane index, ether cleavage of GDGTs from selected samples and compound-specific $\delta^{13}\text{C}$ of the released phytane and biphytanes.

Sample	$\delta^{13}\text{C}$ (‰, PDB)					MI
	phytane	biphytane a	biphytane b	biphytane c	biphytane d	
Core08_401 cm	-31.20	-22.42	-23.49	-20.37	-17.18	0.242
Core08_701 cm	-30.24	-22.01	-20.64	-19.75	-19.64	0.209
Core10_01 cm	-34.46	-23.23	-28.76	-20.71	-20.39	0.239
Core10_41 cm	-43.60	-89.93	-83.29	-52.23	-20.20	0.805
Core10_71 cm	-51.29	-61.04	-61.00	-28.65	-18.93	0.532
Core10_121 cm	-60.20	-100.96	-96.13	-81.62	-22.24	0.942

Biphytane a is the structure with no cyclopentane ring. It is likely released from GDGT-0 and GDGT-1. Biphytane b has one cyclopentane ring, therefore, it could originate from either GDGT-1, GDGT-2 or GDGT-3. The two-ring structure in biphytane c points to the linkage with GDGT-3 and crenarchaeol. Finally, biphytane d can be produced by crenarchaeol and its isomer.

As we discussed previously, ANME group preferentially synthesizing cyclized GDGTs. If we want to trace the potential carbon flow from methane to the microbial community, the $\delta^{13}\text{C}$ of biphytane b might be the best choice because it represents all GDGTs with 1 to 3 cyclopentane rings. All of the four biphytane structures have been identified and their compound-specific carbon isotopes have been determined and showed in Table 4.3. But we only use the $\delta^{13}\text{C}$ from biphytane b as representation.

The correlation between methane index and $\delta^{13}\text{C}$ of biphytane b for MC 118 samples is shown in Fig. 4.6. Linear regression shows that there is a perfect linear correlation between samples's MI and the $\delta^{13}\text{C}$ of biphytane b. This clearly illustrates that for a sample with higher MI, there are more ^{13}C depleted archaeal lipids that most likely come from methane. These results demonstrate that methane index is a robust molecular proxy for the gas hydrate destabilization and/or free methane release in the marine environment.

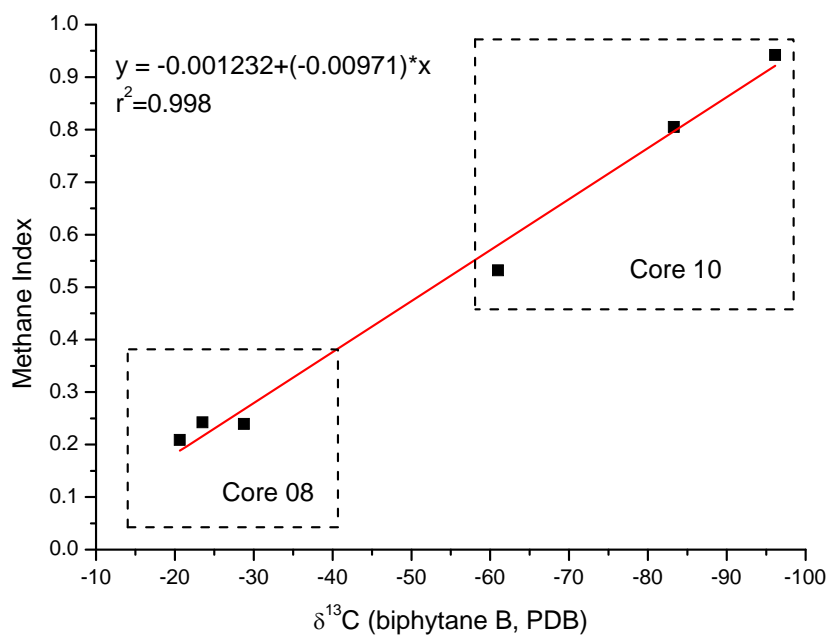


Fig. 4.7. Methane index vs. compound-specific ^{13}C from biphtane b, released from the GDGTs collected from Core 08 and Core 10, MC 118, Gulf of Mexico.

Using Methane Index to Identify Hydrate Impacted Environments

In order to validate the applicability of methane index in detecting the hydrate instability, we collected all published data that is available for both $\delta^{13}\text{C}$ of biphytane b, and MI calculations (Fig. 4.7).

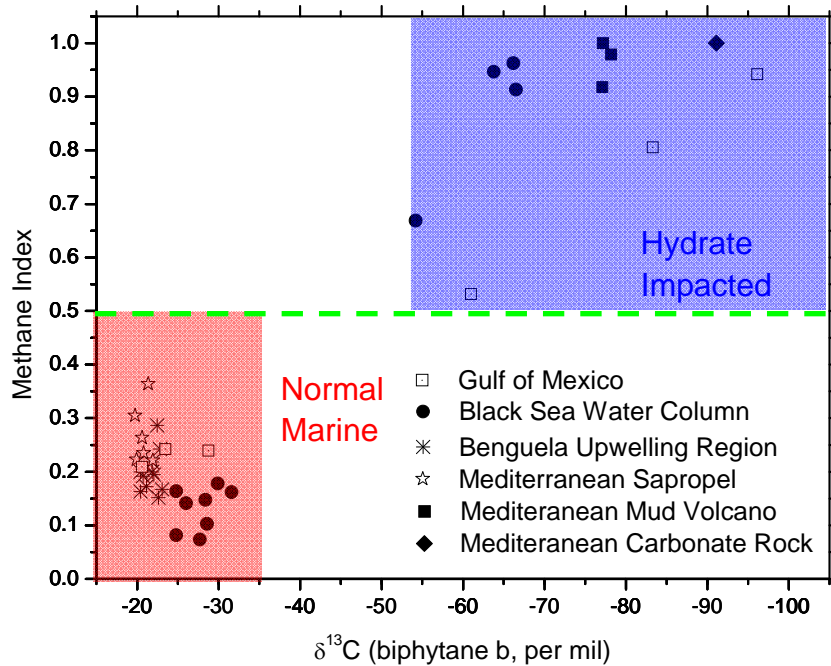


Fig. 4.8. Plot of methane index vs. $\delta^{13}\text{C}$ for the marine environment of (1) Gulf of Mexico (this study), (2) Black Sea water column (Wakeham et al., 2004; Wakeham et al., 2003), (3) Benguela upwelling region (Pancost et al., 2008), (4) Mediterranean sapropel (Pancost et al., 2008), (5) Mediterranean mud volcano (Pancost et al., 2001), and Mediterranean carbonate rocks (Bouloubassi et al., 2006). Two areas can be identified based on the spatial distribution of all data points: (1) “Normal Marine” with MI smaller than 0.5 and $\delta^{13}\text{C}$ greater than -35 ‰ and (2) “Hydrate Impacted” with MI greater than 0.5 and $\delta^{13}\text{C}$ smaller than -55 ‰.

The above plot was composed of samples from a variety of locations like Gulf of Mexico (this study) , Black Sea water column (Wakeham et al., 2004; Wakeham et al., 2003), Benguela upwelling regions (Pancost et al., 2008), Mediterranean sapropel (Pancost et al., 2008), Mediteranean mud volcano (Pancost et al., 2001), and Mediteranean carbonate rocks (Bouloubassi et al., 2006). Two areas blocks are defined based on their MI and $\delta^{13}\text{C}$: (1) the “Normal Marine” block with MI smaller than 0.5 and $\delta^{13}\text{C}$ greater than -35 ‰ and (2) “Hydrate Impacted” block with MI greater than 0.5 and $\delta^{13}\text{C}$ smaller than -55 ‰. It seems that 0.5 is a reasonable number to separate hydrate impacted samples from normal marine samples.

Application of Methane Index in Environmental Samples

To see how this methane index works we established a data base which contains all published GDGT data in marine environments that are also available to us, and calculated their methane index. According to the environment where the samples come from, we classified them as “Normal Marine” and “Possibly Impacted by Gas Hydrates” and made the histogram plot for the two environments in Fig. 4.8.

The “Normal Marine” exhibit Gauss distribution-like pattern with all samples have their MI less than 0.5, and the highest abundance occur between 0.2 and 0.3. For the “Possibly Impacted by Gas Hydrates” samples, some samples have MI smaller than 0.5, but a larger number of them have MI greater than 0.5, and the highest one even reaches 1. These are the samples from the gas hydrate dissociation and/or free methane gas venting environments where methanotrophic ANME group of archaea abundantly occur. Their

contribution to the GDGT pool left fingerprints in these lipid biomarkers, and can be retrieved through the methane index reconstruction.

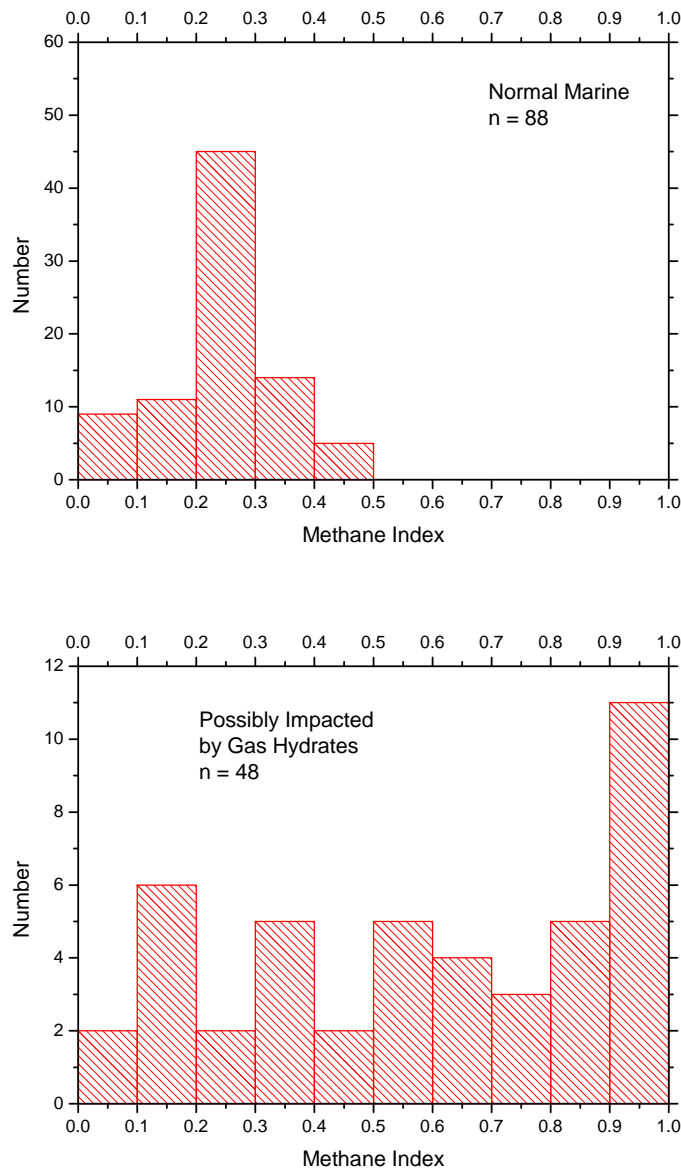


Fig. 4.9. Histogram shows the methane index calculated from a number of different marine environments. “Normal Marine” is comprised of samples from Arabian Sea, Bermuda Time Series sites, Black Sea, equatorial Pacific, Mediterranean (Turich et al., 2007), Santa Monica Basin, Santa Barbara Basin (Pearson et al., 2001), Cariaco Basin (Lea et al., 2003), Gulf of Mexico (Pi et al., 2009), Hawaii (Ingalls et al., 2006), Benguela

upwelling region, and Mediterranean sapropel (Pancost et al., 2008). “possibly Impacted by Gas Hydrates” is comprised of Black Sea water column (Wakeham et al., 2004; Wakeham et al., 2003), Gulf of Mexico MC 118 (Pi et al., 2009), Mediterranean cold seep (Pancost et al., 2001), and Mediterranean carbonate rocks (Bouloubassi et al., 2006).

Chapter 4

Concluding Remarks

In this study we constructed the “Methane Index”, which is an archaeal tetraether lipid biomarker index designed to detect the instability of marine gas hydrates in the geological past. The rationales of this proxy are the observation in hydrate impacted and/or free gas venting environments, abundant methanotrophic ANME group of archaea would contribute significant amount of lipids to the GDGT pool, which will characterize the GDGT profile with exceptionally high concentrations of GDGT-1, GDGT-2 and GDGT-3. Detailed study in two sediment cores from the Gulf of Mexico show that MI correlates well with pore water chemistry and stable isotopes of carbonate minerals. Further validation of this proxy comes from the compound-specific $\delta^{13}\text{C}$ analysis of the GDGT-released biphytanes. Samples with higher MI correlate to lower $\delta^{13}\text{C}$, indicating greater methane impact. In addition, this comparison also shows that 0.5 might be a good cut off number to distinguish hydrate impacted samples, from normal marine seawater or sedimentation. Application of MI for existing GDGT data from known environment corroborated the idea that MI, in combination with carbon isotopes of biphytane, is a powerful tool in detecting hydrate dissociation and/or free methane release. Given the fact the gas hydrate destabilization is paramount for Earth’s climate in the geological past and possibly in the future, the application of this methane index may be an effective tool in paleoceanography, paleoclimatology and paleobiology studies.

References

- Barnes, R.O., and Goldberg, E.D., 1976, Methane production and consumption in anoxic marine sediments: *Geology*, v. 4, p. 297-300.
- Bioetius, A., Ravensschlag, K., Schubert, C.J., Rickert, D., Widdel, F., Cleseke, A., Amann, R., Jorgensen, B.B., Witte, U., and Pfannkuche, O., 2000, A marine microbial consortium apparently mediating anaerobic oxidation of methane: *Nature*, v. 407, p. 623-626.
- Blumenberg, M., Seifert, R., Reichart, G.J., Pape, T., and Michaelis, W., 2004, Membrane lipid patterns typify distinct anaerobic methanotrophic consortia: *Proceedings of the National Academy of Sciences of the United States of America*, v. 101, p. 11111-11116, DOI:10.1073/pnas.0401188101.
- Bouloubassi, I., Aloisi, G., Pancost, R.D., Hopmans, E., Pierre, C., and Sinninghe Damste, J.S., 2006, Archaeal and bacterial lipids in authigenic carbonate crusts from eastern Mediterranean mud volcanoes: *Organic Geochemistry*, v. 37, p. 484-500.
- Brocks, J.J., and Pearson, A., 2005, Building the biomarker tree of life: *Reviews in Mineralogy and Geochemistry*, v. 59, p. 233-258.
- Cannariato, K.G., and Stott, L.D., 2004, Evidence against clathrate-derived methane release to Santa Barbara Basin surface waters?: *Geochemistry Geophysics Geosystems*, v. 5, doi:10.1029/2003GC000600.
- de Garidel-Thoron, T., Beaufort, L., Bassinot, F., and Henry, P., 2004, Evidence of large

- methane releases to the atmosphere from deep-sea gas-hydrate dissociation during the last glacial episode: *Proceedings of the National Academy of Sciences of the United States of America*, v. 101, p. 9187-9192.
- DeLong, E.F., 1992, Archaea in coastal marine environments: *Proceedings of the National Academy of Sciences of the United States of America*, v. 89, p. 5685-5689.
- Dickens, G.R., O'Neil, J.R., Rea, D.K., and Owen, R.M., 1995, Dissociation of oceanic methane hydrate as a cause of the carbon isotope excursion at the end of the Paleocene: *Paleoceanography*, v. 10, p. 965-971.
- Eglinton, T.I., and Eglinton, G., 2008, Molecular proxies for paleoclimatology: *Earth and Planetary Science Letters*, v. 275, p. 1-16.
- Formolo, M.J., Lyons, T.W., Zhang, C.L., Kelley, C., Sassen, R., Horita, J., and Cole, D.R., 2004, Quantifying carbon sources in the formation of authigenic carbonates at gas hydrate sites in the Gulf of Mexico: *Chemical Geology*, v. 205, p. 253-264.
- Forster, A., Schouten, S., Baas, M., and Sinnighe Damste, J.S., 2007, Mid-Cretaceous (Albian-Santonian) sea surface temperature record of the tropical Atlantic Ocean: *Geology*, v. 35, p. 919-922, DOI: 10.1130/G23874A.1.
- Francis, C.A., Roberts, K.J., Beman, J.M., Santoro, A.E., and Oakley, B.B., 2005, Ubiquity and diversity of ammonia-oxidizing archaea in water columns and sediments of the ocean: *Proceedings of the National Academy of Sciences of the United States of America*, v. 102, p. 14683-14688, 10.1073/pnas.0506625102.

- Fuhrman, J.A., McCallum, K., and Davis, A.A., 1992, Novel major archaeobacterial group from marine plankton: *Nature*, v. 356, p. 148-149.
- Hinrichs, K.U., Hayes, J.M., Sylva, S.P., Brewer, P.G., and DeLong, E.F., 1999, Methane-consuming archaeobacteria in marine sediments: *Nature*, v. 398, p. 802-805.
- Hopmans, E.C., Schouten, S., Pancost, R.D., van der Meer, M.T.J., and Sinnighe Damste, J.S., 2000, Analysis of intact tetraether lipids in archaeal cell material and sediments by high performance liquid chromatography/atmospheric pressure chemical ionization mass spectrometry: *Rapid Communications in Mass Spectrometry*, v. 14, p. 585-589.
- Huguet, C., Kim, J.H., Damste, J.S.S., and Schouten, S., 2006, Reconstruction of sea surface temperature variations in the Arabian Sea over the last 23 kyr using organic proxies (TEX86 and U-37(K')): *Paleoceanography*, v. 21, DOI: 10.1029/2005PA001215.
- Ingalls, A.E., Shah, S.R., Hansman, R.L., Aluwihare, L.I., Santos, G.M., Druffel, E.R.M., and Pearson, A., 2006, Quantifying archaeal community autotrophy in the mesopelagic ocean using natural radiocarbon: *Proceedings of the National Academy of Sciences of the United States of America*, v. 103, p. 6442-6447, 10.1073/pnas.0510157103.
- Jiang, G., Kennedy, M.J., and Christie-Blick, N., 2003, Stable isotopic evidence for methane seeps in Neoproterozoic postglacial cap carbonates: *Nature*, v. 426, p.

822-826.

Jiang, G.Q., Shi, X.H., and Zhang, S.H., 2006, Methane seeps, methane hydrate destabilization, and the late Neoproterozoic postglacial cap carbonates: Chinese Science Bulletin, v. 51, p. 1152-1173.

Jiang, H.C., Dong, H.L., Yu, B.S., Ye, Q., Shen, J., Rowe, H., and Zhang, C.L., 2008, Dominance of putative marine benthic archaea in Qinghai Lake, north-western China: Environmental Microbiology, v. 10, p. 2355-2367.

Karner, M.B., DeLong, E.F., and Karl, D.M., 2001, Archaeal dominance in the mesopelagic zone of the Pacific Ocean: Nature, v. 409, p. 507-510.

Kennett, J.P., Cannariato, K.G., Hendy, I.L., and Behl, R.J., 2000, Carbon Isotopic Evidence for Methane Hydrate Instability During Quaternary Interstadials: Science, v. 288, p. 128-133.

—, 2002, Methane hydrates in Quaternary climate change: The Clathrate Gun hypothesis: Washington, DC, American Geophysical Union.

Koga, Y., Morii, H., Akagawa-Matsushita, M., and Ohga, M., 1998, Correlation of polar lipid composition with 16S rRNA phylogeny in methanogens: Further analysis of lipid component parts: Bioscience Biotechnology and Biochemistry, v. 62, p. 230-236.

Koga, Y., Nishihara, M., Morii, H., and Akagawa-Matsushita, M., 1993, Ether polar lipids of methanogenic bacteria: Structures, comparative aspects, and biosynthesis: Microbial Review, v. 57, p. 164-182.

- Konneke, M., Bernhard, A.E., de la Torre, J.R., Walker, C.B., Waterbury, J.B., and Stahl, D.A., 2005, Isolation of an autotrophic ammonia-oxidizing marine archaeon: *Nature*, v. 437, p. 543-546.
- Kvenvolden, K.A., 1999, Potential effects of gas hydrate on human welfare: Proceedings of the National Academy of Sciences of the United States of America, v. 96, p. 3420-3426.
- Lea, D.W., Pak, D.K., Peterson, L.C., and Hughen, K.A., 2003, Synchronicity of tropical and high-latitude Atlantic temperatures over the last glacial termination: *Science*, v. 301, p. 1361-1364.
- Liu, Z., Pagani, M., Zinniker, D., DeConto, R., Huber, M., Brinkhuis, H., Shah, S.R., Leckie, R.M., and Pearson, A., 2009, Global Cooling During the Eocene-Oligocene Climate Transition: *Science*, v. 323, p. 1187-1190, 10.1126/science.1166368.
- Padden, M., Weissert, H., and de Rafelis, M., 2001, Evidence for late Jurassic release of methane from gas hydrate: *Geology*, v. 29, p. 223-226.
- Pancost, R.D., Coleman, J.M., Love, G.D., Chatzi, A., Bouloubassi, I., and Snape, C.E., 2008, Kerogen-bound glycerol dialkyl tetraether lipids released by hydrolysis of marine sediments: A bias against incorporation of sedimentary organisms?: *Organic Geochemistry*, v. 39, p. 1359-1371, 10.1016/j.orggeochem.2008.05.002.
- Pancost, R.D., Hopmans, E.C., Sinnighe Damste, J.S., and Party, T.M.S.S., 2001, Archaeal lipids in Mediterranean Cold Seeps: Molecular proxies for anaerobic

- methane oxidation: *Geochimica Et Cosmochimica Acta*, v. 65, p. 1611-1627.
- Pancost, R.D., Zhang, C.L., Tavacoli, J., Talbot, H.M., Farrimond, P., Schouten, S., Damste, J.S.S., and Sassen, R., 2005, Lipid biomarkers preserved in hydrate-associated authigenic carbonate rocks of the Gulf of Mexico: *Palaeogeography Palaeoclimatology Palaeoecology*, v. 227, p. 48-66.
- Pearson, A., Huang, Z., Ingalls, A.E., Romanek, C.S., Wiegel, J., Freeman, K.H., Smittenberg, R.H., and Zhang, C.L., 2004, Nonmarine crenarchaeol in Nevada hot springs: *Applied and Environmental Microbiology*, v. 70, p. 5229-5237.
- Pearson, A., McNichol, A.P., Benitez-Nelson, B.C., Hayes, J.M., and Eglinton, T.I., 2001, Origins of lipid biomarkers in Santa Monica Basin surface sediment: A case study using compound-specific Delta C-14 analysis: *Geochimica Et Cosmochimica Acta*, v. 65, p. 3123-3137.
- Pearson, A., Pi, Y.D., Zhao, W.D., Li, W.J., Li, Y.L., Inskeep, W., Perevalova, A., Romanek, C.S., Li, S.G., and Zhang, C.L., 2008, Factors controlling the distribution of archaeal tetraethers in terrestrial hot springs: *Applied and Environmental Microbiology*, v. 74, p. 3523-3532.
- Pi, Y.D., Ye, Q., Jiang, H.C., Wang, P., Li, S.G., Noakes, J., Culp, R., Dong, H.L., and Zhang, C.L., 2009, Archaeal lipids and 16S rRNA gene characterizing non-hydrate and hydrate-impacted sediments in the Gulf of Mexico: *Geomicrobiology Journal*, v. 26, p. 1-11.
- Powers, L.A., Werne, J.P., Johnson, T.C., Hopmans, E.C., Sinnighe Damste, J.S., and

- Schouten, S., 2004, Crenarchaeotal membrane lipids in lake sediments: A new paleotemperature proxy for continental paleoclimate reconstruction?: *Geology*, v. 32, p. 613-616.
- Reeburgh, W.S., 1976, Methane consumption in Cariaco Trench waters and sediments: *Earth and Planetary Science Letters*, v. 28, p. 337-344.
- Sassen, R., Roberts, H.H., Carney, R., Milkov, A.V., DeFreitas, D.A., Lanoil, B., and Zhang, C.L., 2004, Free hydrocarbon gas, gas hydrate, and authigenic minerals in chemosynthetic communities of the northern Gulf of Mexico continental slope: relation to microbial processes: *Chemical Geology*, v. 205, p. 195-217, 10.1016/j.chemgeo.2003.12.032.
- Sassen, R., Roberts, H.H., Jung, W., Lutken, C.B., DeFreitas, D.A., Sweet, S.T., and Guinasso, N.L., 2006, The Mississippi Canyon 118 gas hydrate site: A complex natural system, *Offshore Technology Conference*: Houston, TX.
- Schouten, S., Hopmans, E.C., Baas, M., Boumann, H., Standfest, S., Konneke, M., Stahl, D.A., and Sinnighe Damste, J.S., 2008, Intact membrane lipids of "Candidatus *Nitrosopumilus maritimus*," a cultivated representative of the cosmopolitan mesophilic Group I Crenarchaeota: *Applied and Environmental Microbiology*, v. 74, p. 2433-2440.
- Schouten, S., Hopmans, E.C., Forster, A., van Breugel, A., Kuypers, M.M.M., and Sinnighe Damste, J.S., 2003, Extremely high sea-surface temperatures at low latitudes during the middle Cretaceous as revealed by archaeal membrane lipids:

- Geology, v. 31, p. 1069-1072.
- Schouten, S., Hopmans, E.C., Pancost, R.D., and Sinnighe Damste, J.S., 2000, Widespread occurrence of structurally diverse tetraether membrane lipids: Evidence for the ubiquitous presence of low-temperature relatives of hyperthermophiles: Proceedings of the National Academy of Sciences of the United States of America, v. 97, p. 14421-14426.
- Schouten, S., Hopmans, E.C., Schefuss, E., and Damste, J.S.S., 2002, Distributional variations in marine crenarchaeotal membrane lipids: a new tool for reconstructing ancient sea water temperatures?: Earth and Planetary Science Letters, v. 204, p. 265-274.
- Sinnighe Damste, J.S., Ossebaar, J., Abbas, B., Schouten, S., and Verschuren, D., 2009, Fluxes and distribution of tetraether lipids in an equatorial African lake: Constraints on the application of the TEX86 palaeothermometer and BIT index in lacustrine settings: Geochimica Et Cosmochimica Acta, v. 73, p. 4232-4249.
- Stadnitskaia, A., Nadezhkin, D., Abbas, B., Blinova, V., Ivanov, M.K., and Sinnighe Damste, J.S., 2008, Carbonate formation by anaerobic oxidation of methane: Evidence from lipid biomarker and fossil 16S rRNA: Geochimica Et Cosmochimica Acta, v. 72, p. 1824-1836.
- Stott, L.D., Bunn, T., Prokopenko, M., Mahn, C., Gieskes, J., and Bernhard, J.M., 2002, Does the oxidation of methane leave an isotopic fingerprint in the geologic record?: Geochemistry Geophysics Geosystems, v. 3,

doi:10.1029/2001GC000196.

Turich, C., Freeman, K.H., Bruns, M.A., Conte, M., Jones, A.D., and Wakeham, S.G., 2007, Lipids of marine Archaea: Patterns and provenance in the water-column and sediments: *Geochimica Et Cosmochimica Acta*, v. 71, p. 3272-3291, 10.1016/j.gca.2007.04.013.

Wagner, T., Wallmann, K., Herrle, J.O., Hofmann, P., and Stuesser, I., 2007, Consequences of moderate ~25,000 yr lasting emission of light CO₂ into the mid-Cretaceous ocean: *Earth and Planetary Science Letters*, v. 259, p. 200-211.

Wakeham, S.G., Hopmans, E.C., Schouten, S., and Sinnighe Damste, J.S., 2004, Archaeal lipids and anaerobic oxidation of methane in euxinic water columns: a comparative study of the Black Sea and Cariaco Basin: *Chemical Geology*, v. 205, p. 427-442.

Wakeham, S.G., Lewis, C.M., Hopmans, E.C., Schouten, S., and Sinnighe Damste, J.S., 2003, Archaea mediate anaerobic oxidation of methane in deep euxinic waters of the Black Sea: *Geochimica Et Cosmochimica Acta*, v. 67, p. 1359-1374.

Wang, J.S., Jiang, G.Q., Xiao, S.H., Li, Q., and Wei, Q., 2008, Carbon isotope evidence for widespread methane seeps in the ca. 635 Ma Doushantuo cap carbonate in south China: *Geology*, v. 36, p. 347-350, DOI: 10.1130/G24513A.1.

Weijers, J.W.H., Schouten, S., van der Donker, J.C., Hopmans, E.C., and Sinnighe Damste, J.S., 2007, Environmental controls on bacterial tetraether membrane lipid distribution in soils: *Geochimica Et Cosmochimica Acta*, v. 71, p. 703-713.

- Wuchter, C., Schouten, S., Coolen, M.J.L., and Sinnighe Damste, J.S., 2004, Temperature-dependent variation in the distribution of tetraether membrane lipids of marine Crenarchaeota: Implications for TEX86 paleothermometry: *Paleoceanography*, v. 19, DOI:10.1029/2004PA001041.
- Zachos, J., Pagani, M., Sloan, L., Thomas, E., and Billups, K., 2001, Trends, rhythms, and aberrations in global climate 65 Ma to present: *Science*, v. 292, p. 686-693.
- Zhang, C.L., Pancost, R.D., Sassen, R., Qian, Y., and Macko, S.A., 2003, Archaeal lipid biomarkers and isotopic evidence of anaerobic methane oxidation associated with gas hydrates in the Gulf of Mexico: *Organic Geochemistry*, v. 34, p. 827-836, 10.1016/s0146-6380(03)00003-2.
- Zhang, C.L., Pearson, A., Li, Y.L., Mills, G., and Wiegel, J., 2006, Thermophilic temperature optimum for crenarchaeol synthesis and its implication for archaeal evolution: *Applied and Environmental Microbiology*, v. 72, p. 4419-4422.
- Zhang, C.L.L., and Lanoil, B., 2004, Geomicrobiology and biogeochemistry of gas hydrates and cold seeps: *Chemical Geology*, v. 205, p. 187-194, 10.1016/j.chemgeo.2004.01.001.
- Zhang, C.L.L., Li, Y.L., Wall, J.D., Larsen, L., Sassen, R., Huang, Y.S., Wang, Y., Peacock, A., White, D.C., Horita, J., and Cole, D.R., 2002, Lipid and carbon isotopic evidence of methane-oxidizing and sulfate-reducing bacteria in association with gas hydrates from the Gulf of Mexico: *Geology*, v. 30, p. 239-242.